Journal of Molecular Catalysis A: Chemical 330 (2010) 10–17

Contents lists available at ScienceDirect

Journal of Molecular Catalysis A: Chemical

journal homepage: www.elsevier.com/locate/molcata

Effect of La_2O_3-dopping on the Al_2O_3 supported cobalt catalyst for Fischer-Tropsch synthesis

Zhe Cai [a], Jinlin Li [a,*], Kongyong Liew [b], Juncheng Hu [a]

[a] Key Laboratory of Catalysis and Materials Science of the State Ethnic Affairs Commission & Ministry of Education, South-Central University for Nationalities, Wuhan, China
[b] Faculty of Industrial Science and Technology, University Malaysia Pahang, 26500 Kuantan, Malaysia

ARTICLE INFO

Article history:
Received 26 March 2010
Received in revised form 23 June 2010
Accepted 25 June 2010
Available online 3 July 2010

Keywords:
Fischer-Tropsch synthesis
La_2O_3-doped Al_2O_3
Cobalt

ABSTRACT

Alumina was doped with lanthana, La_2O_3, by either impregnation or co-precipitation. The doped and undoped alumina was then used as supports for the preparation of cobalt catalysts by incipient wetness impregnation. The catalysts prepared were characterized by nitrogen adsorption–desorption, powder X-ray diffraction, hydrogen temperature programmed reduction, hydrogen temperature programmed desorption, O_2-titration and diffuse reflectance infrared Fourier transform spectroscopy, and the catalytic properties for Fischer-Tropsch synthesis (FTS) have been evaluated. The results showed that La_2O_3-dopping impacted the catalytic performance significantly. The catalyst with the La_2O_3-doped support prepared by co-precipitation showed better reducibility, activity and product selectivities. The higher ratio of the octahedral to tetrahedral cobalt species of the co-precipitated catalyst relative to the catalyst doped by impregnation might have caused the enhanced performance. The presence of the hydrocarbonyl species, distinguished by its vibrational feature, is directly related to CO conversion and chain-growth.

1. Introduction

Fischer-Tropsch synthesis (FTS) attracts much attention as an option for producing clean transportation fuels and chemicals by conversion of natural gas or coal [1,2]. Cobalt-based catalysts are some of the most important candidates for FTS to produce high molecular weight paraffinic waxes that can be hydrocracked to produce lubricants and diesel fuels [3]. To increase the number of cobalt active sites, the cobalt is dispersed as clusters on high surface area supports such as SiO_2, TiO_2 or Al_2O_3. Alumina is often used due to its favorable mechanical properties [4]. Previous studies indicated that cobalt supported on alumina was not completely reduced to the metallic state because of significant metal-support interactions [3,5]. Chen and Zhang [6] found that when the metal loading was lower than the dispersion capacity in the γ-Al_2O_3 supported transition metal (Ni, Co or Cu) oxide catalysts, the supported M^{2+} ions were preferentially incorporated into the tetrahedral vacancies of γ-Al_2O_3, and that the amount of M^{2+} ions incorporated into the octahedral vacancies increased with increased M^{2+} loading. Since octahedral M^{2+} ions are easier to be reduced to the metallic state than the tetrahedral M^{2+} ions, researchers [7] tried to increase the octahedral ratio of the M^{2+} (Ni^{2+} in the study) to increase the degree of reduction. Similarly, many researchers [8–10] reported that the octahedrally coordinated cobalt FTS catalyst could also be more easily reduced than the cobalt in the tetrahedral environment and hence, display better catalytic properties. Rare earth metal oxides are often used as promoters in cobalt [11–13] and iron [14] based CO hydrogenation catalysts (e.g., FTS [15]). Vada et al. [12] studied a La^{3+}/Co/Al_2O_3 system and found that La^{3+} increased the overall activity and chain-growth probability when a low La^{3+} loading was used. Ren et al. [16] studied NiO/Al_2O_3 catalysts with La^{3+} promoter, and found that the dispersed La^{3+} species on γ-Al_2O_3 increased the ratio of octahedral Ni^{2+} ions to the tetrahedral ones, and thus increased the degree of reduction of the catalysts. Ledford et al. [13] studied two methods of preparing lanthanum promoted Co/Al_2O_3 catalysts. They observed promotional effects only when La^{3+} was impregnated first followed by cobalt, and for higher La^{3+} loadings, a La–Co mixed oxide was suggested to be formed and, in turn, enhanced the dispersion of cobalt. In the present study, a support was prepared by co-precipitation consisting of γ-Al_2O_3 doped with La_2O_3 and then it was subsequently loaded with cobalt. It was expected that when the lanthana was used as a dopant, a greater fraction of octahedral sites will be formed on the surface of γ-Al_2O_3 crystallites and provide sites for Co ions during impregnation. Also, it was anticipated that the co-precipitation procedure would favor octahedral site formation relative to the case of impregnating the lanthana, hence displacing Co to the preferred octahedral sites providing a more facile reduction. In this contribution, a series of lanthana doped alumina supports was prepared by impregnation or co-precipitation. Cobalt was added to both the La_2O_3-doped and undoped alumina by incipient wetness impregnation. The following techniques were used to characterize the catalysts, including

* Corresponding author. Tel.: +86 027 67843016; fax: +86 027 67842752.
E-mail addresses: lij@mail.scuec.edu.cn, jinlinli@hotmail.com (J. Li).

1381-1169/$ – see front matter © 2010 Elsevier B.V. All rights reserved.
doi:10.1016/j.molcata.2010.06.025

nitrogen adsorption–desorption, powder X-ray diffraction (XRD), hydrogen temperature programmed reduction (H_2-TPR), hydrogen temperature programmed desorption (H_2-TPD) and O_2-titration and diffuse reflectance infrared Fourier transform spectroscopy (DRIFTS). FTS reaction tests were carried out using a fixed bed reactor.

2. Experimental

2.1. Catalyst preparation

2.1.1. Preparation of supports

The La_2O_3-doped alumina support was prepared by co-precipitation as follows: known amounts of aluminum nitrate and lanthamum nitrate solutions were mixed in appropriate proportions. Ammonium hydroxide was added to the mixed solution to precipitate the hydroxide. The pH value of the solution was kept constant at 9.0 ± 0.1. The obtained support is denoted as LAP (2.9 wt% La_2O_3). Alumina support without La_2O_3 prepared by co-precipitation was labeled as AP.

The support with the same loading of La_2O_3 was also prepared by incipient wetness impregnation with the desired amount of aqueous lanthanum nitrate on AP. The excess water was evaporated in a rotary evaporator at around 363 K. This support was named LAI. A commercial La_2O_3-doped support (SASOL Germany GmbH), labeled as LAS, was used as a reference. All the materials were dried in an oven overnight at 393 K, crushed, and sieved to obtain 120 mesh particles, followed by calcination at 1023 K for 6 h.

2.1.2. Preparation of cobalt catalysts

The 12 wt% cobalt catalysts were prepared by impregnating the different synthesized supports with aqueous solutions of cobalt nitrate. The samples were dried at 393 K and calcined in air at 623 K for 6 h, hereafter denoted as CAP, CLAI, CLAS and CLAP.

2.2. Catalyst characterization

2.2.1. Powder X-ray diffraction

The X-ray diffraction (XRD) measurements for the samples were carried out using a Brukers D8 powder X-ray diffractometer with monochromatic CuKα radiation and a VANTEC-1 detector over a 2θ range of 20–80° with a step size of 0.0167°, and from 35° to 40° with a step size of 0.008° steps for the crystallite size of cobalt oxide. The in situ XRD measurement was carried out as follows. The sample, placed in the XRK 900 reactor chamber (Anton paar) mounted on a goniometer, was first purged with pure nitrogen at 423 K for 1 h to flush away water and impurities. Pure hydrogen gas was introduced to the cell after cooling to room temperature. The temperature was then increased to 723 K at a rate of 1 K/min, followed by several scans taken in an interval of 1 h between scans. The sample temperature and reduction gas admitted into the in situ cell were reliably controlled and measured. The crystallite phase was detected by comparing the patterns with those in the standard powder XRD file compiled by the Joint Committee on Powder Diffraction Standards (JCPDS). The average Co_3O_4 crystallite size was calculated by line broadening analysis using the Scherrer equation [17].

2.2.2. BET surface area and pore size distribution

The BET surface area and pore size distribution were measured by nitrogen adsorption–desorption at the boiling temperature of nitrogen (77 K) using a Quantachrome Autosorb-1-C-MS. Before the measurement, the samples were outgassed at 473 K for >6 h. The surface area was obtained by applying the Brunauer–Emmett–Teller (BET) model for adsorption in a relative pressure range of 0.05–0.30. The total pore volume of each sample was calculated from the amount of N_2 vapor adsorbed at a relative pressure of 0.99. Pore size distributions were evaluated from the desorption branches of the isotherms using the Barrett–Joyner–Halenda (BJH) model.

2.2.3. Hydrogen temperature programmed reduction

The reduction profiles of the catalysts were measured by hydrogen temperature programmed reduction (H_2-TPR) experiments employing a Zeton Altamira AMI-200 unit. Calcined catalysts (~0.10 g) were placed in a U-shape quartz reactor, with a thermocouple for continuous temperature measurement. Samples were first pretreated by flowing high purity argon at 423 K, and cooled to 323 K, to remove water or other residual contaminants. Then, 10% H_2/Ar (constant flow rate of 30 ml/min) was switched on and the temperature was raised from 323 to 1073 K at a rate of 10 K/min, and held for 30 min at 1073 K. Hydrogen consumption was monitored using a thermal conductivity detector (TCD).

2.2.4. Hydrogen temperature programmed desorption

The dispersion and crystallite size of cobalt were measured by hydrogen temperature programmed desorption (H_2-TPD) using a U-shaped quartz reactor and the Zeton Altamira AMI-200 unit. The catalysts (~0.15 g) were reduced at 723 K for 12 h and cooled to 373 K in flowing hydrogen. Prior to increasing the temperature from 373 to 723 K at a rate of 10 K/min, the samples were held at 373 K for 1 h under an argon stream to drive away weakly bound physisorbed species. Then the catalysts were held at 723 K under flowing argon to desorb the remaining chemisorbed hydrogen; meanwhile, the TCD detector began to record the signal until it returned to the baseline. The amount of desorbed hydrogen was calculated by comparing the integrated TPD spectrum with the mean areas of calibrated hydrogen pulses. The formula for the calculation has been shown in previous works [18].

2.2.5. O_2-titration

The degree of reduction was measured by O_2-titration done in the Zeton Altamira AMI-200 unit. The samples which had been reduced in pure hydrogen at 723 K for 12 h were reoxidized at 723 K by introducing pulses of high purity oxygen, until there was no further consumption of O_2, detected by the thermal conductivity detector located downstream. The reference gas for TCD was high purity helium. All flow rates were set to 30 ml/min. The extent of catalyst reduction was calculated assuming stoichiometric reoxidation of Co to Co_3O_4. The formula for the calculation is described elsewhere [18].

2.2.6. Diffuse reflectance infrared Fourier transform spectroscopy (DRIFTS)

Adsorption properties of catalysts were measured by in situ DRIFTS with a Nicolet NEXUS 6700 FTIR instrument. The spectral resolution was 4 cm^{-1} and 32 scans were obtained for each spectrum. The DRIFTS unit contains a mercury cadmium telluride (MCT) detector, and a diffuse reflectance attachment was used. High purity carbon monoxide (>99.9%) and syngas (H_2/CO = 2) served as probe gases. Nitrogen (>99.999%) was used as the purge gas and hydrogen (>99.999%) was used as the reducing gas. The gases were cleaned prior to use by passing through gas purifiers. The catalysts (30–40 mg) were placed in an infrared cell with ZnSe windows and reduced in situ at 723 K for 10 h under atmospheric pressure in a hydrogen stream at a flow rate of 20 ml/min. After the reduction procedure, the system was cooled to the desired temperature and the background spectra were recorded before the introduction of probe gases. Each spectrum was referenced to a spectrum of the catalyst collected at the desired temperature under H_2 flow before CO or syngas adsorption. Circulating water was used to cool the body of the reaction chamber. A thermocouple located directly in the sample was used for temperature control.

Table 1
Surface area, average pore diameter and pore volume.

Sample	Surface area (m^2/g)	Pore volume (cm^3/g)	Average pore diameter (nm)	Crystallite diameter (nm)[a]
AP	168.8	0.438	7.81	–
LAI	160.0	0.417	9.58	–
LAS	143.9	0.548	12.37	–
LAP	199.7	0.497	7.81	–
CAP	143.6	0.335	7.86	14.02
CLAI	127.7	0.306	9.55	14.14
CLAS	121.9	0.430	12.38	14.17
CLAP	173.2	0.377	7.81	14.49

[a] Average Co_3O_4 particle diameter obtained from XRD line broadening analysis.

2.3. Catalytic evaluation

FTS was performed in a fixed bed reactor (id = 12 mm) at 503 K and 1.0 MPa. The catalysts (ca. 0.5 g) were mixed with 5 g of carborundum to minimize the temperature gradient and reduced in situ with H_2 at atmosphere pressure. With H_2 flowing (6 NL h^{-1} g^{-1}, 298 K, 0.1 MPa), the reactor temperature was raised from room temperature to 373 K at 2 K/min, increased to 723 K at a rate of 1 K/min, and held for 10 h. The reactor was then cooled to 373 K. At that temperature, syngas, with space velocity of 4 SL g^{-1} h^{-1} (273 K, 0.1 MPa), was switched on and the pressure was increased to 1.0 MPa. The reactor temperature was increased to 503 K in 16 h and the reaction was performed at 503 K. The reaction products were collected after more than 80 h of operation to achieve a good mass balance at close to steady state, typically. The carbon monoxide conversion and hydrocarbon selectivities were measured at steady state conditions over the period of operation. The discharged gases were analyzed online by an Agilent MicroGC 3000A gas chromatograph (GC). The analysis of the liquid product, which was collected in the cold trap (269 K), was performed using an Agilent 6890N GC equipped with a flame ionization detector (FID). The solid wax, which was collected in the hot trap (373 K), was analyzed using an Agilent 7890A GC.

3. Results and discussion

3.1. BET surface area and porosity

The surface area, average pore diameter and pore volume data of the supports and the cobalt catalysts are listed in Table 1. Lanthana dopping has a marginal influence on the pore volume. However, the porosity of the supports was significantly affected by the preparation method. The co-precipitation method (LAP support) resulted in the highest BET surface area, while the commercial support (LAS) gave the lowest surface area but the widest average pore size. As can be seen in Table 1, La_2O_3-dopping by the method of impregnation increased the average pore diameter from 7.81 nm (for undoped alumina support AP) to 9.58 nm (LAI), indicating that the impregnation of lanthana caused some blocking of the narrower pores relative to undoped AP. The impregnation with cobalt lowered both the support surface area and the pore volume, and did not change the average pore size, which suggests that some cobalt species have entered the pore of the supports.

3.2. X-ray diffraction results

XRD patterns of the catalysts are presented in Fig. 1. The diffraction peaks at 45.7° and 66.6° are attributed to the γ-Al_2O_3 support and the peaks at 31.4°, 36.9°, 45.0°, 59.5° and 65.5° are assigned to the Co_3O_4 phase, which exists on all the catalysts [15]. The diffraction peak of La_2O_3 phase could not be detected from the XRD patterns of catalysts, indicating that the La_2O_3 was highly dispersed on the support [19]. The size data of the Co_3O_4 crystallites are shown in Table 1. Crystallite size of Co_3O_4 increased slightly on dopping with La_2O_3, suggesting that La_2O_3 may have influenced the Co_3O_4 crystal growth.

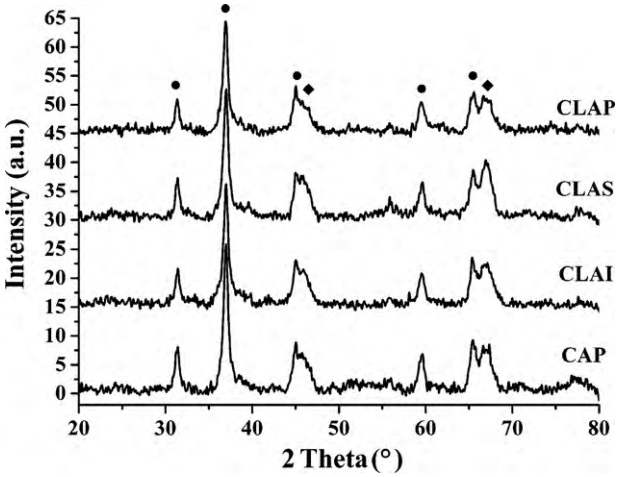

Fig. 1. X-ray diffraction patterns for calcined catalysts (●: Co_3O_4; ♦: γ-Al_2O_3).

The in situ XRD patterns of catalysts reduced at 723 K under H_2 are shown in Figs. 2–5. For all the catalysts, the reduction with H_2 at 723 K for 5 h resulted in the reduction of most of the Co_3O_4 to metal Co. When the reduction temperature reached 573 K, the Co_3O_4 phase of all the catalysts transformed to CoO, indicating that Co_3O_4 reduction is fast regardless of the support composition and structure. However, the diffraction peaks of Co metal for catalysts doped with La_2O_3 can be found immediately as soon as the temperature reached 723 K, but for CAP (without La_2O_3-dopping), these peaks appeared only after having been reduced at 723 K for 1 h. The relative peak intensity of the reduced cobalt in the catalyst doped with La_2O_3 was higher than the undoped catalyst, which suggests that dopping with La_2O_3 enhanced the reduction of CoO phase to Co. For all catalysts except CLAP, peaks of CoO are still found even after reduction in H_2 at 723 K for 5 h. It is concluded that CLAI showed similar reduction properties to that of CLAS, and CLAP exhibited the highest extent of reduction.

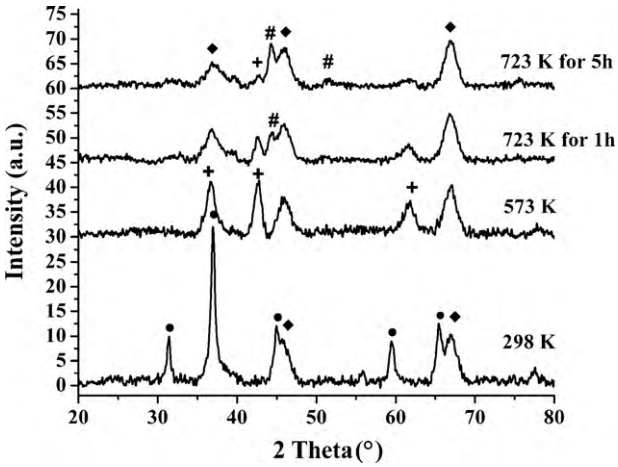

Fig. 2. In situ X-ray diffraction patterns of CAP catalyst reduced in pure H_2 (●: Co_3O_4; ♦: γ-Al_2O_3; +: CoO; #:Co^0).

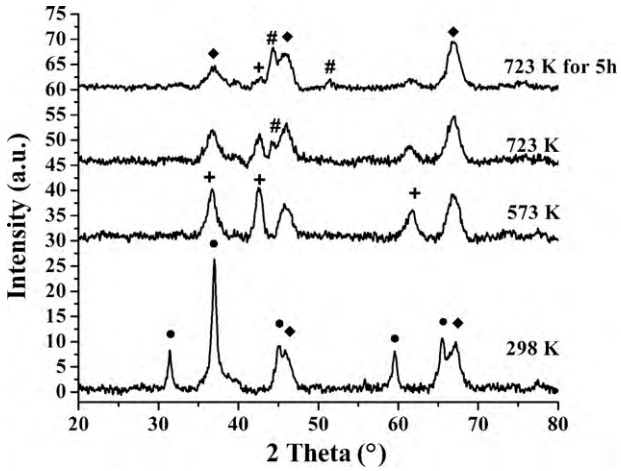

Fig. 3. In situ X-ray diffraction patterns of CLAI catalyst reduced in pure H_2 (●: Co_3O_4; ♦: γ-Al_2O_3; +: CoO; #:Co^0).

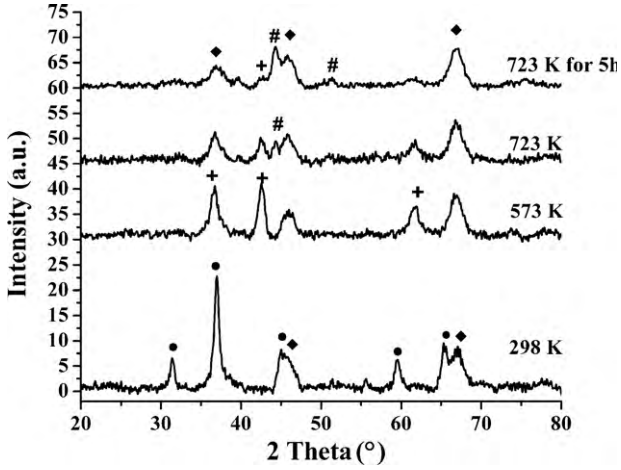

Fig. 4. In situ X-ray diffraction patterns of CLAS catalyst reduced in pure H_2 (●: Co_3O_4; ♦: γ-Al_2O_3; +: CoO; #:Co^0).

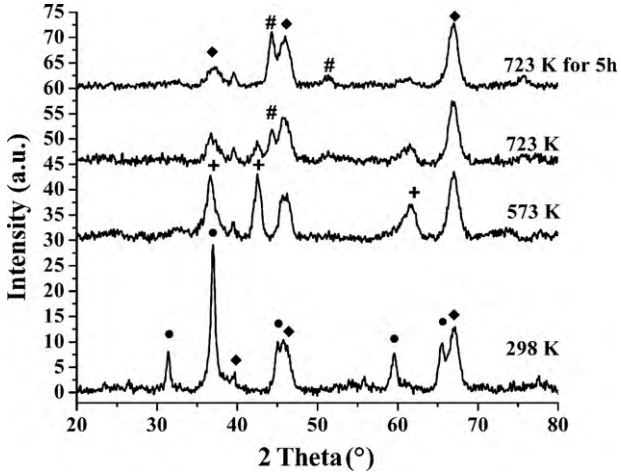

Fig. 5. In situ X-ray diffraction patterns of CLAP catalyst reduced in pure H_2 (●: Co_3O_4; ♦: γ-Al_2O_3; +: CoO; #:Co^0).

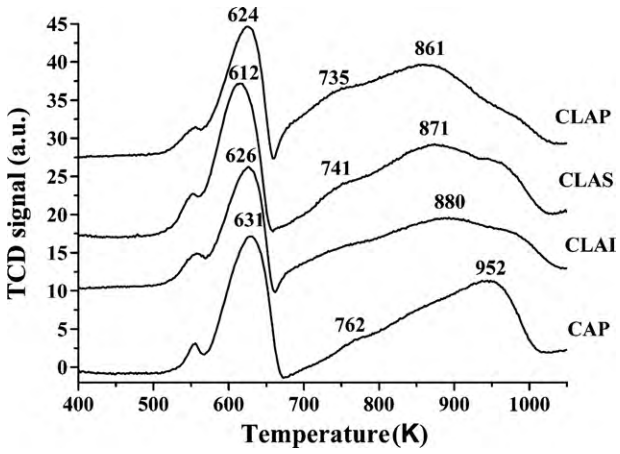

Fig. 6. TPR spectra of calcined catalysts.

3.3. H_2-temperature programmed reduction

The TPR spectra of catalysts are shown in Fig. 6. Three reduction peaks for Co/Al_2O_3 are observed at temperature ranges of <573, 573–673 and >673 K, respectively. The peak at 573–673 K is attributed to the reduction of Co_3O_4 to CoO [17]. The broad peak at high temperature (>673 K) is ascribed to the subsequent reduction of CoO to Co^0 [20]. The appearance of the peaks at the different reduction temperature suggests that all catalysts exhibited the different interactions between the metal and support [21,22]. Besides two main reduction peaks, a small peak is observed below 573 K. This peak could be attributed to the reductive decomposition of residual $Co(NO_3)_2$ [23]. The reduction process was consistent with the results of in situ XRD.

Table 2 presents the reduction degree calculated from the TPR profile. All the Co_3O_4 can be reduced to Co^0 in the whole temperature program process for CLAP, In the temperature range above 673 K, assuming the H_2 consumption to completely reduce CoO to Co to be 2.04 mmol/gcatal, CoO was reduced to Co metal completely for catalyst CLAP, while for the other catalysts, 70–86% of the CoO could be reduced by the amount of H_2 above this temperature. This is due to the lower reducibility of these cobalt species with stronger interaction with the supports. It is noticed that the reduction degree of catalyst CLAP was above 100% which may be caused by the H_2 consumption of the nitrate ions.

All reduction peaks of CAP appeared at higher reduction temperature than the catalysts doped with La_2O_3, indicating that La_2O_3-dopping increased catalyst reducibility. The methods of La_2O_3-dopping markedly affected the reduction properties of Co/Al_2O_3 catalysts. It should be noted that the second reduction step (>673 K) of several catalysts comprised of broad peaks, which may be due to different degrees of interaction between cobalt and the support [24]. Also, the existence of cobalt aluminate cannot be excluded, as it typically reduces at or above 1273 K. The reduction

Table 2
Reduction degree and H_2 consumption for the TPR profile calculation.

Catalysts	H_2 consumption for the peak <673 K (mmol/gcat)	H_2 consumption for the peak >673 K (mmol/gcat)	H_2 consumption for 373–1073 K (mmol/gcat)	Reduction degree (%)[a]
CAP	0.62	1.43	2.05	76
CLAI	0.70	1.68	2.38	88
CLAS	0.72	1.75	2.47	91
CLAP	0.82	2.03	2.85	105

[a] H_2 consumption should be 2.72 mmol/gcat to reduce the Co_3O_4 to the metal cobalt.

Table 3
H_2-temperature programmed desorption and O_2 pulse reoxidation results for catalysts.

Sample	$H_{2\ desorbed}$ (μmol/g)	$d_{uncorrected}$ (%)[a]	$D_{uncorrected}$ (nm)[b]	O_2 uptake (μmol/g)	$d_{corrected}$ (%)[c]	Reducibility (%)	$D_{corrected}$ (nm)[d]
CAP	183.2	17.99	5.7	579.3	42.37	42.46	2.4
CLAI	189.0	18.56	5.6	734.3	34.49	53.82	3.0
CLAS	193.5	19.00	5.4	736.8	35.19	54.00	2.9
CLAP	197.5	19.39	5.3	813.6	32.51	59.64	3.2

[a] The uncorrected catalyst dispersion.
[b] The uncorrected cobalt metal cluster diameter.
[c] The corrected catalyst dispersion.
[d] The corrected cobalt metal cluster diameter.

peak above 673 K shifted to a lower temperature for catalyst CLAP compared with the catalysts CLAI and CLAS, and the intensity of this broad peak increased. All the above results indicated that CLAP exhibits the best reduction properties among the catalysts studied.

3.4. H_2-temperature programmed desorption and O_2-oxidation

Table 3 presents the H_2-temperature programmed desorption and O_2-oxidation data. The La_2O_3-dopping increased the degree of reduction of the catalysts significantly, and the method of La_2O_3-dopping affected the metal cobalt cluster size, dispersion and reducibility. Catalyst reducibility increased in the order of CLAI, CLAS to CLAP. Furthermore, the cobalt cluster size was increased by the dopping of La_2O_3 and was slightly affected by the dopping method. Khassin et al. [9] reported that the Co^{2+} cations which entered the support structure and occupied the octahedral positions could be reduced at lower temperature. For Mg^{2+} and Zn^{2+} promoted catalysts, promoter cations occupied the tetrahedral sites of the supports and caused the Co^{2+} cations to occupy mainly octahedral sites, thus increasing the extent of reduction of the catalyst. Catalyst performance parameters of the promoted catalysts were significantly better than the unpromoted catalysts. In the present work, it could be considered that in CLAP, the La_2O_3-dopping process carried out at the same time with the formation of γ-Al_2O_3 crystallite phase and the dispersed lanthanum species on γ-Al_2O_3 might inhibit the incorporation of cobalt species from entering the tetrahedral sites of γ-Al_2O_3. When the La_2O_3-dopping process was carried out after the formation of the support crystallite phase in the CLAI catalyst, the impregnated La_2O_3 could not inhibit the tetrahedral sites to the same degree as in the CLAP catalyst, and thus the CLAI catalyst exhibited a lower degree of reduction relative to the CLAP catalyst [6,9,10]. Similar finding was reported by Ren et al. [16] in their studies of La_2O_3 promoted NiO/Al_2O_3 in which they found from the UV–VIS DRS, XRD and TPR results that the dispersed La^{3+} species inhibited the incorporation of Ni^{2+} ions into tetrahedral vacancies on the surface of support and increased the ratio of Ni^{2+} ions incorporated into the octahedral vacancies of γ-Al_2O_3. Khassin et al. [8] studied Co–Al co-precipitated catalysts for FTS, they observed that Co^{2+} occupied mostly the octahedral sites in Mg^{2+} and Zn^{2+} promoted samples, and had higher reducibility and better catalytic performance. The catalysts with cobalt cations in octahedral sites were found to be more active for FTS than those with cobalt cations in tetrahedral sites [9,10].

3.5. Fischer-Tropsch synthesis catalytic tests

Results of the FTS tests are displayed in Table 4. CO conversion and selectivities to heavy hydrocarbons increased with dopping of La_2O_3.The activity of the La_2O_3-doped catalysts increased in the order of CLAI < CLAS < CLAP which is consistent with the order of reducibility. Selectivity for methane showed an opposite trend to the activity. CLAP catalyst displayed the highest FT activity and the lowest methane selectivity among the catalysts studied.

Previous studies on cobalt-based catalysts for FTS found that high reducibility provided more cobalt active sites and hence, increased the CO conversion rate by increasing the active site density [25–30]. In the present work, lanthanum oxide facilitated the reduction of cobalt oxide dispersed on the supports, and the impact was more significant in the case of the CLAP catalyst leading to an increase in CO conversion. Methane selectivity was 13.19% for the case of the unpromoted catalyst, CAP; however, with La_2O_3-dopping, methane selectivity decreased significantly to 9.14% for CLAS and 8.05% for CLAP. Vada et al. [12] reported that in the studies of the La^{3+} promotion in the Co/Al_2O_3 catalysts, the promoted La^{3+} decreased the methane selectivity and increase the long chain-growth ability. High methane selectivity has been reported in the case of catalysts possessing low reducibility and high dispersion [31], and is typically attributed to the presence of unreduced cobalt oxides which catalyzed the WGS reaction, resulting in a higher H_2/CO ratio on the surface Co^0 sites, which in turn tends toward the hydrogenation of adsorbed species to lower carbon number product. It should be mentioned that CLAP has the highest reduction degree, and CO_2 selectivity was 0.49%, much lower than those of CLAI (1.50%) and CLAS (1.64%); this lower WGS activity is thus consistent with lower CH_4 selectivity.

3.6. Diffuse reflectance infrared Fourier transform spectroscopy

3.6.1. DRIFTS spectra of CO adsorbed on reduced catalysts at room temperature

The spectra of CO adsorbed on the surface of undoped and La_2O_3-doped catalysts are shown in Fig. 7. The DRIFTS spectra were recorded after reduction of the catalyst in hydrogen, introduc-

Table 4
FTS reaction CO conversion and product distribution.

Catalysts	CO conversion (%)	CO_2 selectivity (%)	Hydrocarbon selectivity (%)				
			CH_4	C_2	C_3	C_4	C_5+
CAP	28.04	1.88	13.19	1.44	2.96	5.26	75.28
CLAI	32.76	1.50	8.57	0.83	2.31	4.01	82.79
CLAS	33.06	1.64	9.14	1.15	2.32	3.99	81.75
CLAP	34.92	0.49	8.05	0.91	2.39	3.81	84.36

The catalysts were reduced in H_2 at 723 K for 10 h before FTS.
Reaction conditions: $H_2/CO = 2$, space velocity of syngas: 4 SL g^{-1} h^{-1} (273 K, 0.1 MPa), temperature: 503 K; pressure: 1.0 MPa.

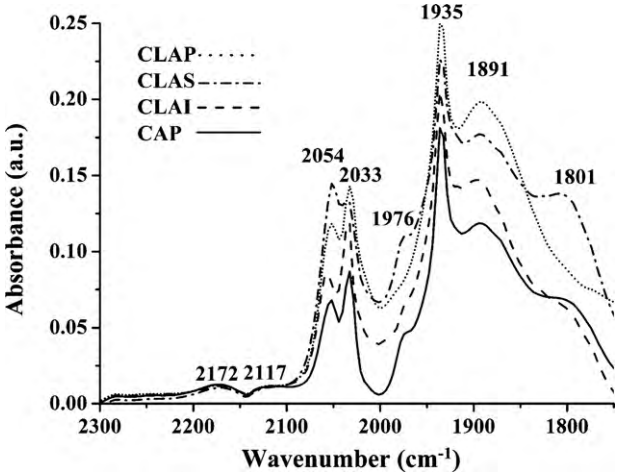

Fig. 7. DRIFTS spectra of CO adsorbed on reduced catalysts at 303 K.

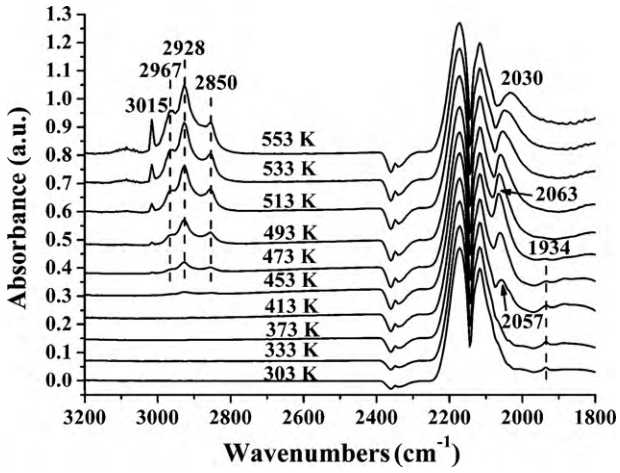

Fig. 9. DRIFTS spectra of syngas reaction on reduced CLAI.

tion of CO at room temperature (~1 h), and purging with flowing N_2.

Several bands located at 2054, 2033, 1976, 1935, 1891, and 1801 cm^{-1} in addition to two broad bands appearing at 2171 and 2120 cm^{-1} could be clearly resolved for all the catalysts. The bands at 2171 and 2120 cm^{-1} have been assigned to residual weakly adsorbed carbon monoxide [32]. The band positioned at 1801 cm^{-1} could be assigned to CO adsorbed on metal cobalt sites [33]. The band at 1891 cm^{-1} arises either from CO adsorbed in a bridged position on Co (0001) or from monocarbonyls adsorbed on defect sites, edges, or corners [34]. The bands located at 1935 and 1976 cm^{-1} are attributed to CO adsorbed on Co^0 in the bridge conformation. It should be noted that the relative intensities of bands positioned at approximately 1891, 1935 and 2033 cm^{-1} correspond to the same trend for CO conversion and the opposing trend towards methane selectivity (see Section 3.5), leading to the speculation that CO adsorbed on the active cobalt phase sites resulted in the high probability for chain growth and low CH_4 selectivity. Previous work [35] reported that similar results were obtained for the in situ DRIFTS on Co/SiO_2 catalysts.

For the band located at around 2060 cm^{-1}, Rygh et al. [36] assigned it to overlapping contributions from $Co(CO)_n$, CoHCO, $Co^{\delta+}$-CO ($0 < \delta < 2$), and CO linearly adsorbed on Co (0001). This band was observed in our previous studies, where we assigned it to CO adsorbed on metallic cobalt sites [35]. In the present work, the intensity of the band at 2054 cm^{-1} for the CLAS catalyst was found to be strongest among all the catalysts. The methane selectivity was the highest in this La_2O_3-doped catalyst, with intermediate activity. We propose that this band was due to multi-carbonyl species on $Co^{\delta+}$ with weak electron-donor properties [37].

3.6.2. DRIFTS spectra of syngas reaction on catalyst surfaces

The DRIFTS spectra corresponding to in situ syngas reaction over reduced catalysts are shown in Figs. 8–11, recorded after catalyst reduction and introduction of syngas ($H_2/CO = 2$). The temperature was raised from 303 to 673 K at a rate of 5 K min^{-1}, and syngas flow rate was 6 ml/min.

The spectra could be divided into four regions. There are four bands in the region of 2800–3100 cm^{-1}, corresponding to the ν(CH) modes of CH_4 (3015 cm^{-1}), CH_3 (2968 cm^{-1}), and CH_2 (2927 and 2864 cm^{-1}) [38–40]. The band at ~2350 cm^{-1} is typical of CO_2, while that at ~2143 cm^{-1} is due to residual gas phase CO. Those in the region 1900–2100 cm^{-1} are linear- and bridge-bonded CO adsorbed on cobalt sites. From the spectra of syngas adsorbed on the catalysts and temperature programmed desorption experiments, the following features are noted:

(1) Hydrocarbon species, located in the region 2800–3100 cm^{-1}, appeared on catalyst CAP at 473 K; which is 20 K higher than for the other catalysts. The intensity of these bands on CLAP and CLAS catalysts increases rapidly with increasing temperature. In contrast, the hydrocarbon band intensities for catalysts CAP

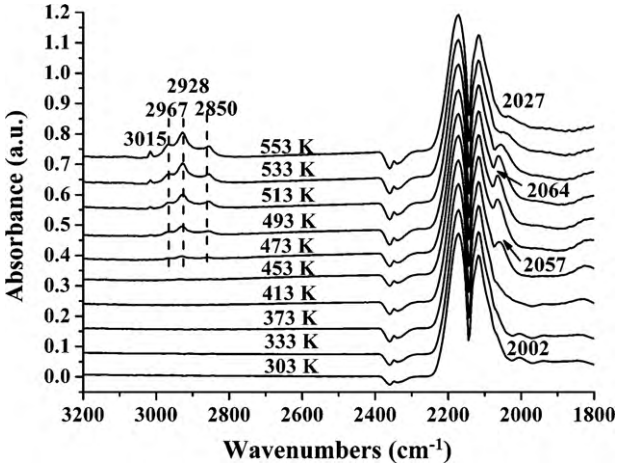

Fig. 8. DRIFTS spectra of syngas reaction on reduced CAP.

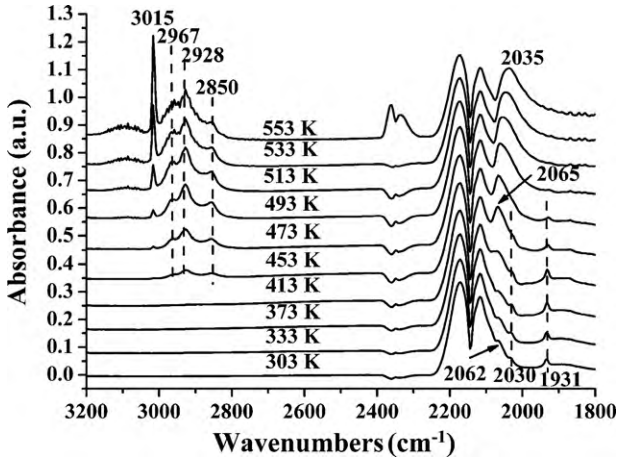

Fig. 10. DRIFTS spectra of syngas reaction on reduced CLAS.

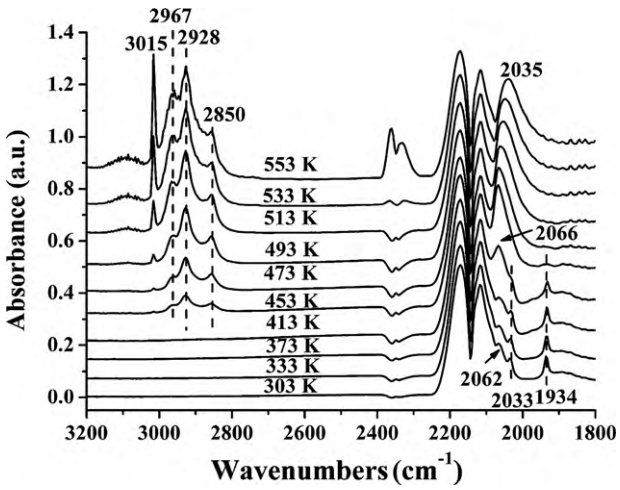

Fig. 11. DRIFTS spectra of syngas reaction on reduced CLAP.

and CLAI were still very weak even at temperature of 553 K. This suggests that CAP and CLAI catalysts have lower initial activity and lower chain-growth probability relative to CLAP and CLAS.

(2) For either CLAP or CLAS, the band intensity of CO_2 (at 2364 and 2338 cm^{-1}) was relatively unchanged in the temperature range of 453–513 K and became stronger at temperatures >533 K, while the bands assigned to hydrocarbon product increased with increasing temperature. These indicate that the products were mainly hydrocarbons and little CO_2 was produced during this heating process. This observation suggests that the temperature range of 453–513 K is appropriate for FT synthesis.

(3) All bands corresponding to linear- and bridge-bonded CO became weaker with increasing temperature, and a new band appeared at around 2060 cm^{-1} at 413 K. As the temperature was increased further, the band shifted to lower wavenumbers to below 2030 cm^{-1} at 553 K. The assignment of the band in the range of 2015–2060 cm^{-1} is still ambiguous since its frequency is close to 2000 cm^{-1}, the dividing line that distinguishes between linear- and bridge-bonded CO absorption. Some researchers [41–43] attributed this new band at 2050–2060 cm^{-1} to a structure of the type HCoCO designated as "hydrocarbonyl". The formation of hydrocarbonyl was assumed to be a prerequisite step in the overall reaction between coadsorbed H_2 and CO. Chen et al. [44] ascribed the new band at 2046 cm^{-1} to "carbonhydride", which was supposed to be formed by coadsorption of CO and H_2 on Co^0 active sites. We also observed a band at around 2015–2029 cm^{-1} on Co/SiO_2 catalysts in previous studies, and ascribed it to hydrocarbonyl species [35]. From the current results, the new band at around 2060 cm^{-1} appeared at 413 K, followed by the appearance of hydrocarbon bands (at the region of 2800–3100 cm^{-1}) at 453 K. The change in intensity of hydrocarbon species is consistent with that of the new band (Fig. 12). It should be pointed out that the new band located at 2020–2060 cm^{-1} is not only directly related to the bands of hydrocarbons (2800–3100 cm^{-1}), but also related to CO conversion and chain-growth. The new band at around 2020–2060 cm^{-1} which is ascribed to the "hydrocarbonyl" species, may be a vibrational feature of some reaction intermediate. With increasing temperature, the intensity of the new band became stronger and shifted to lower wavenumbers, indicating that more hydrocarbonyl species were formed and that the C–O bond became gradually weaker at higher temperatures.

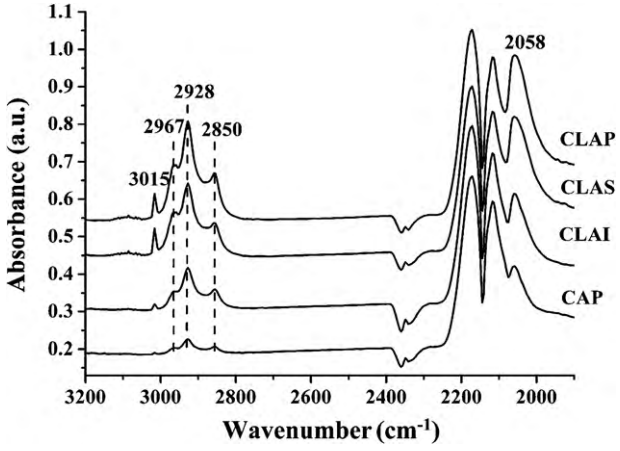

Fig. 12. DRIFTS spectra of syngas adsorbed on reduced catalysts at 503 K.

4. Conclusions

The effect of preparation method of La_2O_3-doped Co/Al_2O_3 FTS catalysts has been investigated by various characterization techniques and catalytic testing using a fixed bed reactor. The following conclusions can be drawn.

(1) The dopping of La_2O_3 strongly influenced the catalytic performance. The Co catalyst with the La_2O_3-doped support prepared by co-precipitation was more easily reducible, resulting in higher FTS activity and lower methane selectivity.

(2) DRIFTS studies show that there is more CO adsorbed on cobalt species for CLAP than the other catalysts; thus, the catalyst displayed higher reducibility, activity, and lower methane selectivity. The intensity of bands corresponding to CO adsorbed on the catalysts with different supports follows the order of CLAP > CLAS > CLAI > CAP, which is consistent with the order of CO conversion for FT synthesis and the product selectivities.

(3) The intensity of the band attributed to hydrocarbonyl species showed a direct relationship with both CO conversion and chain-growth for the CLAP catalyst, while CAP and CLAI displayed lower initial activity and chain-growth probability relative to CLAP and CLAS.

Acknowledgement

Financial support from National Natural Science Foundation of China (Grant Nos: 20590360 and 20773166) are gratefully acknowledged.

References

[1] H. Schulz, Appl. Catal. 186 (1999) 3–12.
[2] R.B. Anderson, Fischer-Tropsch Synthesis, Academic Press, NY, 1984.
[3] G. Jacobs, T.K. Das, Y.Q. Zhang, J.L. Li, G. Racoillet, B.H. Davis, Appl. Catal. A 233 (2002) 263–281.
[4] E. Iglesia, S.L. Soled, R.A. Fiato, G.H. Via, J. Catal. 143 (1993) 345–368.
[5] W.J. Wang, Y.W. Chen, Appl. Catal. 77 (1991) 223–233.
[6] Y. Chen, L.F. Zhang, Catal. Lett. 12 (1992) 51–62.
[7] S.B. Ren, J.H. Qiu, C.Y. Wang, B.L. Xu, Y.N. Fan, Y. Chen, Chin. J. Catal. 28 (2007) 651–656.
[8] A.A. Khassin, T.M. Yurieva, G.N. Kustiva, L.M. Plyasova, I.S. Itenberg, M.P. Demeshkina, G.K. Chermashentseva, V.F. Anufrienko, V.I. Zaikovskii, T.V. Larina, I.Y. Molina, V.N. Parmon, J. Mol. Catal. A 168 (2001) 209–224.
[9] A.A. Khassin, T.M. Yurieva, G.N. Kustiva, I.S. Itenberg, M.P. Demeshkina, T.A. Krieger, L.M. Plyasova, G.K. Chermashentseva, V.N. Parmon, J. Mol. Catal. A 168 (2001) 193–207.
[10] A.A. Khassin, T.M. Yurieva, V.V. Kaichev, V.I. Bukhtiyarov, A.A. Budneva, E.A. Paukshtis, V.N. Parmon, J. Mol. Catal. A 175 (2001) 189–204.
[11] J. Barrault, A. Guilleminot, Appl. Catal. 21 (1989) 307–312.
[12] S. Vada, B. Chen, J.G. Goodwin, J. Catal. 153 (1995) 224–231.

[13] J.S. Ledford, M. Houalls, A. Proctor, D.M. Hercules, J. Phys. Chem. 93 (1989) 6770–6777.
[14] A.N. Pour, S.M.K. Shahri, H.R. Bozorgzadeh, Y. Zamani, A. Tavasoli, M.A. Marvast, Appl. Catal. A 348 (2008) 201–208.
[15] G.J. Haddad, B. Chen, J.G. Goodwin, J. Catal. 161 (1996) 274–281.
[16] S.B. Ren, J.H. Qiu, C.Y. Wang, B.L. Xu, Y.N. Fan, Y. Chen, Chin. J. Inorg. Chem. 23 (2007) 1021–1028.
[17] B.D. Cullity, Elements of X-ray Diffraction, third ed., Additon-Wesley, Reading. MA, 1967.
[18] Y.H. Zhang, H.F. Xiong, K.Y. Liew, J.L. Li, J. Mol. Catal. 237 (2005) 172–181.
[19] B. Jongsomjit, J. Panpranot, J.G. Goodwin, J. Catal. 215 (2003) 66–77.
[20] A. Bao, K.Y. Liew, J.L. Li, J. Mol. Catal. A 304 (2009) 47–51.
[21] G. Jacobs, Y. Ji, B.H. Davis, D. Cronauer, A.J. Kropf, C.L. Marshall, Appl. Catal. A: Gen. 333 (2007) 177–191.
[22] G. Jacobs, M.C. Ribeiro, W. Ma, Y. Ji, S. Khalid, P.T.A. Sumodjo, B.H. Davis, Appl. Catal. A: Gen. 361 (2009) 137–151.
[23] A. Lapidus, A. Krylova, V. Kazanskii, V. Borovkov, A. Zaitsev, J. Rathousky, A. Zukal, M. Jancalkova, Appl. Catal. 73 (1991) 65–81.
[24] Ø. Borg, E.A. Blekkan, S. Eri, D. Akporiaye, B. Vigerust, E. Rytter, A. Holmen, Top. Catal. 45 (2007) 39–43.
[25] A. Martinez, C. Lopez, F. Marquez, I. Diaz, J. Catal. 220 (2003) 486–499.
[26] J.L. Zhang, J.G. Chen, J. Ren, Y.H. Sun, Appl. Catal. A 243 (2003) 121–133.
[27] A.R. Belamble, R. Oukaci, J.G. Goodwin, J. Catal. 166 (1997) 8–15.
[28] J.L. Li, N.J. Coville, Appl. Catal. A 181 (1999) 201–208.
[29] Y. Wang, M. Noguchi, Y. Takahashi, Y. Ohtsuka, Catal. Today 68 (2001) 3–9.
[30] A.Y. Khodakov, R. Bechara, A. Griboval-Constant, Stud. Surf. Sci. Catal. 142 (2002) 1133–1140.
[31] R.C. Reuel, C.H. Bartholomew, J. Catal. 85 (1984) 63–77.
[32] S.L. Sun, K. Fujimoto, N. Tsubaki, M. Yamada, Catal. Commun. 4 (2003) 361–364.
[33] P. Concepcion, C. Lopez, A. Martinez, V.F. Puntes, J. Catal. 228 (2004) 321–332.
[34] G.Z. Bian, A. Oonuki, Y. Kobayashi, N. Koizumi, M. Yamada, Appl. Catal. A 219 (2001) 13–24.
[35] D.C. Song, J.L. Li, Q. Cai, J. Phys. Chem. C 111 (2007) 18970–18979.
[36] L.E.S. Rygh, O.H. Ellestad, P. Klaeboe, Phys. Chem. Chem. Phys. 2 (2000) 1835–1846.
[37] L. Ji, J. Lin, H.C. Zeng, J. Phys. Chem. B 104 (2000) 1783–1790.
[38] M.J. Heal, E.C. Leisegang, R.G. Torrington, J. Catal. 51 (1978) 314–325.
[39] F.M.T. Mendes, C.A.C. Perez, F.B. Noronha, C.D.D. Souza, D.V. Cesar, H.J. Freund, M. Schmal, J. Phys. Chem. B 110 (2006) 9155–9163.
[40] V. Curtis, C.P. Nicolaides, N.J. Coville, D. Hildebrandt, D. Glasser, Catal. Today 49 (1999) 33–40.
[41] G. Kadinov, C. Bonev, S. Todorova, A. Palazov, J. Chem. Soc. Faraday Trans. 94 (1998) 3027–3031.
[42] E.L. Rodrigues, J.M.C. Bueno, Appl. Catal. 232 (2002) 147–158.
[43] S.Z. Todorova, G.B. Kadinov, Res. Chem. Intermediat. 28 (2002) 291–301.
[44] Y.Q. Chen, M.C. Gong, X.H. Zhu, H. Ming, S.H. Tang, Chem. J. Chin. Univ. 4 (2002) 715–717.